Published in final edited form as:
Biomaterials. 2014 March ; 35(10): 3243–3251. doi:10.1016/j.biomaterials.2013.12.081.

Creating Polymer Hydrogel Microfibres with Internal Alignment *via* Electrical and Mechanical Stretching

Shuming Zhang[a,b,c], **Xi Liu**[a,d], **Sebastian F. Barreto-Ortiz**[c,e,f], **Yixuan Yu**[g], **Brian Ginn**[a,b,c], **Nicholas DeSantis**[a], **Daphne L Hutton**[b,c,h], **Warren Grayson**[b,c,h], **Fu-Zhai Cui**[d], **Brian A. Korgel**[g], **Sharon Gerecht**[a,c,e,f], and **Hai-Quan Mao**[a,b,c,*]

[a]Department of Materials Science and Engineering, Johns Hopkins University, 3400 N. Charles St., Baltimore, MD 21218, USA

[b]Translational Tissue Engineering Centre, Johns Hopkins University, 400 N Broad Way, Baltimore, MD 21287, USA

[c]Institute for NanoBioTechnology, Johns Hopkins University, 400 N. Charles St., Baltimore, MD 21218, USA

[d]Department of Materials Science and Engineering, Tsinghua University, Beijing 100084, China

[e]Department of Chemical and Biomolecular Engineering, Johns Hopkins University, Baltimore, MD 21218, USA

[f]Johns Hopkins Physical Sciences-Oncology Centre, Johns Hopkins University, Baltimore, MD 21218, USA

[g]Department of Chemical Engineering, University of Texas at Austin, Austin, TX 78712, USA

[h]Department of Biomedical Engineering, Johns Hopkins School of Medicine, Baltimore, MD 21205, USA

Abstract

Hydrogels have been widely used for 3-dimensional (3D) cell culture and tissue regeneration due to their tunable biochemical and physicochemical properties as well as their high water content, which resembles the aqueous microenvironment of the natural extracellular matrix. While many properties of natural hydrogel matrices are modifiable, their intrinsic isotropic structure limits the control over cellular organization, which is critical to restore tissue function. Here we report a generic approach to incorporate alignment topography inside the hydrogel matrix using a combination of electrical and mechanical stretching. Hydrogel fibres with uniaxial alignment were prepared from aqueous solutions of natural polymers such as alginate, fibrin, gelatin, and hyaluronic acid under ambient conditions. The unique internal alignment feature drastically enhances the mechanical properties of the hydrogel microfibres. Furthermore, the facile, organic solvent-free processing conditions are amenable to the incorporation of live cells within the hydrogel fibre or on the fibre surface; both approaches effectively induce cellular alignment. This work demonstrates a versatile and scalable strategy to create aligned hydrogel microfibres from various natural polymers.

Correspondence should be addressed to H.-Q.M. (hmao@jhu.edu).

Keywords

Hydrogel; microstructure; fibrin; alginate; hyaluronic acid

1. Introduction

Previous studies on hydrogels have primarily focused on exploring their mechanical and biochemical versatility [1–4] and elucidating their impact on cellular activities [5–9]. There is a lack of methodologies for engineering *anisotropic* topographical cues in hydrogels to control the 3D spatial patterns of encapsulated cells. As a result, controlling topographically induced cell alignment and migration has not been readily achieved for hydrogel matrices, even though such cellular manipulation on 2D substrates has been shown to be important in controlling cell organization, tissue microarchitecture, and biological function [10–13]. On the other hand, cellular alignment mediated by 2D electrospun micro- and nano-fibre matrices has been shown to effectively promote stem cell differentiation and cellular functions [14,15]. Dispersing solid polymer nanofibres into the hydrogel matrix has been used to generate a composite scaffold [16], however, controlling alignment of the nanofibres inside a hydrogel matrix is challenging. Recently, Kang *et al*. have reported a microfluidic-based alginate hydrogel microfibre with a surface alignment feature produced by solution extrusion through a grooved micro-channel, and demonstrated guided neurite outgrowth for neurons cultured on the surface of the microfibers [17,18]. This alignment cue is only confined to the surface of the microfibre. Zhang *et al*. have generated peptide nanofibre hydrogels with long-range nanofibre alignment through heat-assisted self-assembly of amphiphilic peptide molecules and mechanical shear [19]. The resulting aligned nanofibre “noodles” effectively induced cellular alignment in 3D; nevertheless, this method is only applicable to specific peptide materials.

Since polymer chain alignment can be induced during electrospinning, we hypothesized that similar chain alignment can be induced by electrospinning of an aqueous polymer solution and such an alignment can be fixed by crosslinking, thus generating hydrogel fibres with internal alignment. To enhance polymer chain alignment through mechanical shear, we collected the spinning polymer solution jet on a rotating bath containing crosslinking agents. In this study, we examined feasibility of generating internally aligned hydrogel fibres by combined electrospinning and mechanical stretching (electrostretching) approach, and characterized the internal alignment by X-ray scattering analysis and its effect on the mechanical properties of these hydrogel fibres. We tested the versatility of this method by generating hydrogel microfibres from various water-soluble natural polymers using different crosslinking mechanisms. We then investigated the effect of the alignment cue of these hydrogel fibres on the morphology of cells seeded on fibre surface or encapsulated within the hydrogel microfibres.

2. Materials & methods

2.1 Materials and Reagents

Sodium alginate from brown algae (the viscosity of 2% solution at 25°C is ~250 cps), fibrinogen from bovine plasma and poly(ethylene glycol) (PEO, average Mv *ca.* 4,000 kDa) were purchased from Sigma Aldrich. Methacrylated gelatin was prepared according to a previously reported protocol[21]. Thiol-modified hyaluronic acid (HA) and PEG-diacrylate (PEGDA) was purchased from Glycosan BioSystems Inc. Photo initiator Irgacure 2959 was from CIBA Specialty Chemicals. High voltage power supply was from Gamma High Voltage Research. Direct current permanent magnet motor was from Leeson Electric Corp (Grafton). UV source used was Mineralight Lamp UVGL-25 from UVP LLC.

2.2 Generating Hydrogel Microfibres

To produce alginate hydrogel microfibers using the device shown in Fig. 1A, 2–5 kV voltage, 1.5–3.0 wt% alginate and 0.1–0.6 wt% PEO solution were used. In a circular collection bath, 20–100 mM $CaCl_2$ served to stabilize these alginate hydrogel fibres. With similar flow rates and applied voltages, fibrin, gelatin and HA hydrogel fibre bundles were also prepared. Typically, fibrin hydrogel fibres were produced using an aqueous solution that contains 0.67 wt% fibrinogen, 1.0 wt% sodium alginate and 0.1 wt% PEO. Upon collection, the hydrogel fibres were crosslinked in 50 mM $CaCl_2$ with 5 Units/ml thrombin for 20 min. If necessary, a higher concentration of thrombin can be used to shorten the crosslinking time. Gelatin hydrogel fibres were prepared with 3.2 wt% methacrylated gelatin, 0.9 wt% sodium alginate, 0.1 wt% PEO, and 0.4 wt% photo initiator Irgacure 2959, followed by crosslinking with 50 mM $CaCl_2$ solution for 20 min and then UV-irradiation at λ 365 nm for 10 min. Similarly, HA hydrogel fibres were prepared with 1 wt% thiolated HA, 0.7 wt% alginate and 0.2 wt% PEO, and crosslinked with 50 mM $CaCl_2$ and 1 wt% PEGDA. Table 1 shows the specific conditions for spinning several biopolymer hydrogel fibres. In blend biopolymer fibres, alginate and PEO can be removed by rinsing with 0.25 M sodium citrate or treating with alginase. If cellular components were included in the experiments, solutions can be adjusted to isotonic conditions using glucose and salts.

2.3 SEM Analysis

Hydrogel microfibre samples were first serially dehydrated in 50%, 60%, 70%, 80%, 90%, 95% and 100% ethanol for 15 min in each solution, critical point dried, and then sputter-coated with 8-nm thick Au/Pd. Samples were imaged on a JEOL 6700F field-emission SEM.

2.4 Small and Wide Angle X-ray Scattering

SAXS experiment was performed at the Cornell High Energy Synchrotron Source (CHESS, Ithaca, NY, USA). Dry or wet hydrogel fibres were subjected to 10-sec exposures of the synchrotron beam (λ = 0.11521 nm, beam size: 0.5 mm horizontal × 0.1 mm vertical) for 10 times. A 48 mm × 48 mm 2-D CCD detector with pixel size of 46.9 μm × 46.9 μm was used to collect the scattering data. The averaged intensity readings on each pixel of the detector were recorded and analyzed with fit2D. WAXS experiments were performed using a Rigaku R-Axis Spider Diffractometer with an image plate detector and a graphite monochromator using Cu Kα radiation (λ = 0.15418 nm). The instrument was controlled by Rapid/XRD diffractometer control software (version 2.3.8, Rigaku Americas Corp.). Fibres were grouped into a bundle and secured on the sample stage. Two-dimensional diffraction data were collected for 20 min while rotating the sample stage at 5° per min. The 2D diffraction data were radially integrated with 2DP Spider software (version 1.0, Rigaku Americas Corp.)

2.5 Mechanical Testing

Tensile tests on dry and wet hydrogel fibre bundles were performed with a DMA Q800 unit from TA Instruments. Sample diameters were determined using a light microscope. For wet strings, samples were stretched to break within 30 sec to minimize the effect of water evaporation on measurement. The Young's moduli were calculated within the initial linear region of the stress-strain curves from the tests.

2.6 Cell Seeding and Culture

Cryopreserved ASCs (passage 0) were obtained from Pennington Biomedical Research Center. Cells were thawed and expanded in growth medium containing high glucose DMEM (Invitrogen) with 10% fetal bovine serum (FBS, Atlanta Biologicals), 1% penicillin/streptomycin (Invitrogen), and 1 ng/ml of FGF-2 (PeproTech) for use at later passages.

Human umbilical vein endothelial cells (HUVECs; PromoCell, Heidelberg, German) were used between passages 4–5, cultured in endothelial growth medium EGM (PromoCell), and passaged every 3–4 days with 0.05% trypsin (Invitrogen). Human endothelial colony forming cells (ECFCs; Lonza) were expanded and used for experiments between Passages 5 and 9. ECFCs were expanded in flasks coated with Type I collagen (BD Biosciences) in Endothelial Basal Medium-2 (EBM-2; Lonza) supplemented with EGM-2 Bulletkit (Lonza) and 10% FBS (Hyclone). Media was changed every other day, and cells were passaged every 5 to 7 days with 0.05% trypsin/0.1% ethylenediaminetetraacetic acid (EDTA, Invitrogen), and maintained in a humidified incubator at 37°C in a 5% CO_2 atmosphere. To encapsulate cells in hydrogel microfibres, cells were suspended in polymer solution at a concentration of 250–2000 cells/μl before electrostretching using the spinning parameters described above. Cell-loaded fibres were then collected, transferred into Petri dish with media, and cultured in 5% CO_2 incubator at 37°C. To seed ECFCs on top of hydrogel microfibres, 2×10^6 cells in suspension were added to 5 ml of ECFC media supplemented with 50 ng/mL of VEGF (Pierce) in a tube containing the microfibres. The seeding tube was left on a tumbler (Labquake) for 24 h to enhance cell attachment.

2.7 Confocal Immunofluorescence Microscopy

Live cell labelling was performed with CellTracker™ green CMFDA (Invitrogen). For immuno-fluorescence microscopy imaging, cell-hydrogel fibre constructs were fixed with 3.7% formaldehyde (Fisher Chemical) for 15 min, permeabilized with a solution of 0.1% Triton-X-100 (Sigma-Aldrich) in 3.7% formaldehyde for 10 min, washed with PBS, and incubated for 1 h with mouse anti-human von Willebrand factor (1:100; Dako). After rinsing with PBS for three times, samples were incubated with Alexa 488-conjugated phalloidin (1:40; Invitrogen) and with anti-mouse Alexa Fluor 546 conjugate (1:1000; Invitrogen). After 1 h, samples were rinsed with PBS and counterstained with DAPI (1:1000; Roche Diagnostics) for an additional 10 min. Z-stack and cross-sectional images were obtained and processed on a Zeiss LSM 510 Meta confocal microscope.

3. Results

3.1 Preparation of hydrogel microfibres and versatility of the method

This strategy employs electrical and mechanical stretching to induce polymer chain alignment during spinning of an aqueous polymer solution, followed by rapid chain alignment fixation of the polymer jet via crosslinking (Fig. 1A). The *electrostretching* setup is similar to that of electrospinning with the addition of a grounded, motor-driven rotating disc containing a crosslinking solution as the collecting plate; and the polymer jet is charged with a relatively lower electrical potential of 2–5 kV than typically applied for electrospinning (5–30 kV). In this study, the entire process is conducted using aqueous solutions of biopolymers. For example, a solution of sodium alginate (1.5–3.0 wt%) and poly(ethylene oxide) (PEO, 0.1–0.6 wt%) was charged with 3–5 kV positive potential, and extruded through a syringe needle at a flow rate of 1–3 ml/h. The PEO in the alginate solution serves as a thickening agent to adjust the viscosity of the alginate solution jet [20]. The polymer solution was forced to form a jet by the electrical field and was further stretched upon landing on the rotating disc containing 20–50 mM $CaCl_2$ solution at a collecting distance of 3–6 cm from the needle tip. The diameter of the collected hydrogel fibre could be tuned by adjusting the solution extrusion rate and the angular velocity of the rotating disc, which was controlled to be in the range of 25–80 rpm (at a diameter of 20 cm, this corresponds to a linear velocity of 26–84 cm/sec). The obtained fibre diameter increased with solution extrusion rate and decreased with rotation velocity of the collection disc. The average diameter of individual calcium alginate fibres could be controlled in the range of 17–116 μm by varying the flow rate of alginate (2 wt%)-PEO (0.2 wt%) solution from 0.7 to

7 ml/h at room temperature (Fig. 1B). Hydrogel fibres produced with this process showed highly uniform diameters (Fig. 1C); continuous hydrogel microfibres of any length could be produced (Fig. 1G). Furthermore, the hydrogel microfibres could be grouped together to form fibre bundles of tunable diameters depending on the number of individual fibres used.

We demonstrated the versatility of this approach by preparing internally aligned hydrogel microfibres from several natural polymers (alginate, fibrin, gelatine [21] and hyaluronic acid [22]) using different crosslinking schemes (Fig. 1C–F). We first prepared calcium alginate hydrogel fibres. One important advantage of the calcium alginate hydrogel system is its fast gelation rate. Potter *et al*. have determined the displacement of the crosslinking reaction front in 2 wt% alginate solution to be ~20 μm/sec in a 50 mM $CaCl_2$ crosslinking solution, and 40 μm/sec in 100 mM $CaCl_2$ [23]. In the electrostretching system described above, a 40-μm alginate fibre can be effectively crosslinked in about 0.5–1.0 sec by the $CaCl_2$ solution. This fast crosslinking scheme allows the incorporation of other water-soluble polymers to form polymer blend fibres. Additional enzyme-, UV- or chemical-mediated crosslinking reactions can be used together with calcium ions to further stabilize the hydrogel fibres. For example, thrombin-mediated crosslinking of fibrinogen can be used to form fibrin-alginate blend fibres, UV light can be used to crosslink methacrylated gelatin-alginate fibres, and a Michael-type addition reaction can be used to crosslink thiolated hyaluronic acid-alginate fibres. After crosslinking, alginate and PEO can be removed from the polymer blend hydrogel fibres by washing the fibres with sodium citrate. All of these crosslinking and washing steps are carried out in aqueous buffers under ambient conditions and therefore are cell-compatible.

3.2 Preferential alignment in hydrogel microfibres

These electrostretched hydrogel fibre bundles are mechanically stronger and easier to handle than typical hydrogels of the same composition and dimensions. As a demonstration, we used an electrostretched calcium alginate hydrogel fibre bundle to lift a 10-g metal pillar (Fig. 1I), and also tied two individual alginate gel strings into a micro-knot using forceps (Fig. 1J). On the contrary, bulk alginate hydrogels or alginate fibres prepared with the same concentration of alginate but without employing the stretching process cannot withstand such manipulations. Due to the improved mechanical properties and ease of handling, such hydrogel materials can be easily fabricated into other forms like films, tubes and more (Fig. 1L–M).

To probe the structural origin for enhanced mechanical properties, we conducted birefringence imaging of the electrostretched hydrogel fibres. The extinction of light at the cross-point of fibres (Fig. 1K) indicates strong polymer chain alignment within the hydrogel microfibre bundles. This alignment was further confirmed on critical point-dried hydrogel microfibre bundles utilizing scanning electron microscopy (SEM). As shown in Fig. 2A–C, fibrin, methacrylated gelatin, and thiolated HA hydrogels prepared using bulk mixing and crosslinking steps formed random nanofibre mesh networks. In contrast, the electrostretched hydrogel microfibres exhibited preferential alignment along the fibre axis (Fig. 2D–F). When the crosslinking mechanisms are compatible, multi-component hydrogel microfibres can be produced with similar degree of alignment. Fig. S1 shows a bicomponent hydrogel fibre prepared from thiolated HA and gelatin. Such highly porous and aligned surface texture is also very different from recently developed fibrin microthreads, which are dense and smooth on the surface [24,25]. Grouping of individual fibres into bundles followed by further stretching (usually 30–100% of the initial length) and dehydration resulted in dense microfibres with aligned grooves and surface textures (Fig. 2G–H). These dry fibres can be rehydrated to *ca.* 50–100% of their original diameter depending on their drying processes.

To confirm molecular alignment within the hydrogel fibres, both in dry and wet forms, we analysed their small angle X-ray scattering (SAXS) patterns (Fig. 3A and B), which showed strong anisotropic scattering profiles, indicating preferential orientation along the fibre axis. As a comparison, both dry and wet non-stretched alginate samples gave an isotropic scattering pattern (Fig. 3C). The wide-angle X-ray scattering (WAXS) analysis of dry calcium alginate microfibres also showed a reflection profile that is indicative of an oriented polymer crystalline phase (Fig. 3D). The reflection pattern also confirmed that the polymer chains are oriented preferentially along the microfibre axis indicated by the arrow. Results with fibrin and gelatin strings were similar to that of calcium alginate (Fig. S2).

3.3 Enhanced Young's moduli of the hydrogel fibres due to alignment

The preferential alignment of polymer chains within the microfibres drastically improved mechanical properties of the hydrogel fibres. Fig. 3E–G shows the Young's moduli of dry, wet, and rehydrated hydrogel fibre bundles. While dry fibres had limited capacity to elongate (~3–5% strain at break), wet hydrogel fibres were stretched to more than 100% strain before breaking. As a comparison, hydrogels prepared by bulk mixing showed limited stretchability; an alginate hydrogel ruptured at around 20% strain [26]. The average Young's moduli of dry calcium alginate, fibrin, gelatin and HA fibres were 10.0 GPa, 2.2 GPa, 0.8 GPa, and 3.0 MPa, respectively. For wet fibres prior to the drying step, the Young's moduli were several orders of magnitude lower (717 KPa, 37.3 KPa, 2.6 KPa, and 1.3 KPa, respectively). The moduli of rehydrated fibres fell in between the two sets to 108 MPa, 289 KPa, 4.4 KPa, and 58.5 KPa, respectively. In contrast, the calcium alginate hydrogel strings prepared by simple mixing yielded a tensile modulus of 241 KPa in the same test; and hydrogel strings prepared from other polymers were too weak to test in the same fashion. A recent study on hydrogel microfibres achieved a Young's modulus of 0.73 KPa for 0.5 wt% fibrin hydrogel microfibres (stiffness measured with atomic force microscope) [27]. It is, however, much lower than the 37.3 KPa value measured for our fibrin hydrogel microfibres. The modulus and stiffness of the hydrogel fibres may be further adjusted by varying the concentration of starting materials like alginate and fibrinogen, and crosslinking density. For example, the modulus of wet HA hydrogel microfibres was increased by nearly 100-fold to 115 KPa when bifunctional crosslinker poly(ethylene glycol) diacrylate (PEGDA) was replaced with PEG octaacrylate (PEGOA) resulting in a higher degree of fibre crosslinking. As substrate modulus plays an important role in regulating cellular behaviours like proliferation, migration and differentiation, the ability to tune hydrogel fibre modulus and stiffness over such a wide range makes this hydrogel fibre matrix versatile for a wide range of applications [5,6].

3.4 Cell encapsulation and alignment

The relatively low electrical potential applied to the polymer solution (a measured current of 4–6 μA), the aqueous solutions, and ambient crosslinking conditions make this process compatible with cell encapsulation. Since alginate is not a favourable cell scaffold material due to the lack of cell adhesion moieties, we opted to use the fibrin, gelatin or HA blends for cell culture studies. For example, a solution of fibrinogen, alginate, and PEO was mixed with cells, and subjected to the electrostretching condition as described above. Hydrogel fibres were rapidly crosslinked by the calcium solution in the rotating bath, followed by crosslinking of fibrinogen into fibrin network with thrombin. Similarly, methylated gelatin and thiolated HA can be used instead of fibrinogen and the corresponding crosslinking methods discussed in Fig. 1 will be used (detailed conditions are listed in Table 1). All these crosslinking methods are cell-compatible. After the second crosslinking step, alginate and PEO could be removed with sodium citrate, if a higher degree of porosity is desired.

We next examined the compatibility of the newly developed hydrogel matrix for cell culture. We hypothesized that due to the internal alignment of the polymer matrix, cell alignment can be induced. We first examined the encapsulation of adipose tissue-derived stem cells (ASCs) in a fibrin hydrogel fibre bundle prepared from 0.75 wt% fibrinogen solution. After culturing for 5 days in a humidified incubator at 37°C and 5% CO_2 atmosphere, ASCs remained viable and exhibited an elongated morphology along the fibre axis (Fig. 4A and B).

These biodegradable hydrogel fibres with internal and surface alignment feature may serve as an ideal tubular scaffold to study microvascular formation in culture. We next tested human umbilical vein endothelial cell (HUVEC) culture on a single fibrin-alginate microfibre with an average diameter of 10–25 μm as a scaffold. HUVECs were seeded onto these fibres and quickly reached a high degree of coverage in 2 days (Fig. S3). We then used a larger diameter fibrin fibre with an average diameter of 80 to 130 μm as a microvessel template. Human endothelial colony forming cells (ECFCs), a specific subtype of endothelial progenitor cells harvested from umbilical cord blood with demonstrated angiogenic and proliferative potential [28], were seeded on the microtubular template scaffold and proliferated successfully. By day 5 of culture, F-actin staining revealed a preferential alignment of the ECFC cytoskeleton along the hydrogel fibre axis (Fig. 4C and D). More importantly, ECFCs completely covered the microfibre hydrogel and generated a microtubular structure (Fig. 4E), indicating active proliferation during this culture period (Fig. S4). The differentiated cells expressed mature endothelial marker CD31 and von Willebrand factor (vWF, Fig. 4C and D). These preliminary results highlight the significance of this biodegradable hydrogel scaffold for organized adhesion and differentiation of endothelial progenitor cells toward vascular tube formation.

4. Discussion

We have demonstrated that a high degree of axial alignment of polymer chains inside hydrogel microfibres can be induced by a combination of electrical and mechanical stretching effects. It has previously been reported that a limited degree of polymer chain alignment can be induced during the standard electrospinning process as a result of high speed fibre stretching [29–31]. Physical basis of such alignment has been supported by theoretical models, claiming that a high degree of polymer chain alignment can be achieved during the uniaxial stretching of a polymer solution jet when the Weissenberg number, defined as the product of strain rate $\dot{\varepsilon}$ and the conformational relaxation time λ, is greater than 1 [32]. However, despite the high strain rates (10^4–$10^6 s^{-1}$) commonly used in electrospinning, a high degree of alignment is difficult to achieve in electrospun fibres, likely due to the rapid solidification process under typical spinning conditions, which does not give sufficient time for polymer chains to align [33,34]. Besides the flash drying process, there are additional challenges in using conventional electrospinning process to align polymer chains of water-soluble polyelectrolytes, such as alginate and HA. The counter ions associated with these polyelectrolytes greatly increase the conductivities of the aqueous solutions; for example, the conductivity of 2 wt% alginate in water is 4.34 ms/cm [35], which is much higher than the 76.8 μs/cm value for a typical spinnable aqueous solution of PEO (5 w/v%, MW = 600,000) [36]. This extra capacity to carry charge increases the stretching of the solution in electrical field and leads to easy pinch-off of liquid droplets from the feeding nozzle. It hinders the formation of initial liquid filament necessary for electrospinning of polymer jet [36].

Addition of high molecular weight, electrostatically neutral polymers in the spinning solution has been shown as an effective strategy to delay droplet pinch off from feeding nozzle, and thus lead to the formation of stable liquid filament [37,38]. To improve the

spinnability of water-soluble biopolymers, we added high molecular weight PEO (average Mv *ca.* 4,000 kDa) to biopolymer solution, and showed that this strategy successfully maintained the liquid filament stability during the entire spinning and stretching process. In our electrostretching setup, the average air travel time of biopolymer solution jet is 0.1–0.5 sec before it lands in the receiving bath containing the crosslinking solution. In contrast, the air travel time is *ca.* 0.01 sec for the liquid jet in a typical electrospinning setup before solvent evaporation occurs [39]. The extended jet stretching time allowed alginate chains to have sufficient time to align with the flow. Such alignment is further enhanced by the mechanical stretching conferred by the collection wheel (Fig. 5). Under the electrostretching conditions described above, the alginate solution jet has a strain rate $\dot{\varepsilon}$ of 10–70 s^{-1}. Although this strain rate is not very high, it is compensated by the long relaxation time λ, due to the high molecular weight of biopolymer and PEO, thus achieving a sufficiently high Weissenberg number. This conclusion is supported by our observation that a faster rotating velocity leads to smaller diameter fibres with higher tensile modulus, indicating a higher degree of alignment enhanced by stronger mechanical stretching (Fig. S5). Due to the limited electric potential range applied to biopolymer solution (2–5 kV) necessary to maintain a stable liquid filament during spinning, it is difficult to precisely adjust the strain rate by varying the applied voltage. Therefore, controlling strain rate can be easily achieved by changing the collection wheel rotation speed. In this electrostretching configuration, the mechanical stretching imposed by the rotating wheel is indispensible for generating hydrogel microfibers with high degree of internal alignment.

The success of this method also relies on an effective crosslinking or fixation of the induced polymer chain alignment. Here we have demonstrated four different crosslinking strategies that will be applicable for a wide selection of biopolymers. These crosslinking methods are also complementary so that it is possible to prepare blend fibres with different compositions to afford multi-functionalities—a feature particularly suitable for regulating cell adhesion, tissue compatibility, permeability, and surface conjugation of ligands. More interestingly, the biodegradability of the fibres can be tailored easily by blending polymers with different degrees of sensitivity to hydrolysis and degradative enzymes. The degradation can also be triggered on demand. For example, alginate fibres can be selectively dissolved by treating the fibres with sodium citrate or alginase; fibrin fibres can be specifically degraded by plasmin, collagen or gelatin fibers by collagenase, and HA fibres by hyaluronidase. This property allows for dynamic control of selective degradation of hydrogel fibres.

A particular unique feature of the hydrogel fibres generated by this electrostretching method is the excellent mechanical strength achieved for the hydrogel fibres while maintaining sufficient porosity and water content (>95%). Moreover, the porosity of the electrostretched hydrogel fibres can also be easily tuned by varying the input polymer concentration, composition and crosslinking density. This is in contrast with hydrogel fibres prepared by simple extrusion, in which case polymer solutions are pressed through a small orifice and crosslinked during or after extrusion. Hydrogel fibres produced by these methods do not exhibit a high degree of polymer chain alignment, and are therefore mechanically weak and difficult to handle in comparison with hydrogel fibres produced by electrostretching. One interesting improvement of fibre alignment was reported recently by Chae *et al.* demonstrating a process to mimic silkworm spinning in creating aligned alginate fibres through microfluidic channels. The key step of this process involves spinning alginate solution into a dehydration solution, which makes it incompatible for cell encapsulation [40]. Moreover, alginate hydrogels generated by this method are too dense for long-term culture of encapsulated cells.

In our electrostretching process, the entire spinning and crosslinking steps are conducted in aqueous solutions under ambient conditions, making it particularly amenable to cell

encapsulation inside hydrogel fibres. The low electrical potential (3–5 kV) and low shear also ensures high cell viability in hydrogel fibres (Fig. 4 and Fig. S6). It is worth noting that cells right after spinning remained rounded morphology (Fig. S6), and during the culture phase, cells sensed the internal alignment of the hydrogel fibre, and spread in uniaxial alignment fashion along the fibre alignment direction. The alignment cue can be used as an extrinsic factor to promote cell differentiation *in vitro* and *in vivo* [14,15]. The markedly improved mechanical property of the hydrogel fibres makes it easy to handle in culture and for potential *in vivo* implantation. This type of cell-hydrogel fibre constructs can generate 3D cell structure in aligned fashion that is difficult to achieve using other nanofibre or hydrogel scaffolds. A recent study by Onoe *et al.* reported a method to generate hollow microfibres from alginate using a coaxial microfluidic setup for encapsulation of ECM proteins and cells [27]. These hollow fibres are convenient to generate organized cellular structures at high cell density. Nonetheless, there is no internal alignment induced either in the alginate hydrogel shell or in the core, which contributed to low stiffness of less than 1 KPa for the hydrogel core.

Our data also confirm that the hydrogel fibres are excellent scaffold for engineering microvessels. These hydrogel fibre scaffolds offer the advantages of uniform and controlled fibre diameter, tailorable compositions, surface alignment cue, and tunable degradation property. Fig. 4 highlights an example of such a culture. This construct also facilitates sequential cell seeding, therefore permitting the generation of multi-layered co-culture of endothelial cells and pericytes or smooth muscle cells. By dissolving the hydrogel fibre with specific enzymes, the hollow microvessels can be used as an *in-vitro* capillary culture model.

5. Conclusion

Here we report a scalable platform strategy for the generation of hydrogel microfibres with internal alignment induced by a combination of electrical and mechanical stretching. Using this approach, we have produced hydrogel microfibres with high water content (>95% water) from various biopolymers, including alginate, fibrin, gelatin, hyaluronic acid and their combinations. These microfibres exhibit markedly enhanced mechanical properties as a result of the polymer chain alignment, while maintaining high water content and porosity. The facile preparation conditions are conducive to cell encapsulation in generating “cellular strings”. Due to their biodegradable nature and unique geometry and alignment topography, they are ideal scaffold candidates for generating aligned tissue structures or engineering microvascular tissues with controlled diameters. Preliminary cell culture results demonstrated the great potential and versatility of these hydrogel microfibres to guide cellular orientation and differentiation. The development of these hydrogel fibres represents an important step toward successful fabrication of hierarchically organized cellular structures in 3D.

Supplementary Material

Refer to Web version on PubMed Central for supplementary material.

References

1. Seliktar D. Designing cell-compatible hydrogels for biomedical applications. Science. 2012; 336:1124–8. [PubMed: 22654050]
2. Burdick JA, Anseth KS. Photoencapsulation of osteoblasts in injectable RGD-modified PEG hydrogels for bone tissue engineering. Biomaterials. 2002; 23:4315–23. [PubMed: 12219821]

3. Williams CG, Kim TK, Taboas A, Malik A, Manson P, Elisseeff J. In vitro chondrogenesis of bone marrow-derived mesenchymal stem cells in a photopolymerizing hydrogel. Tissue Eng. 2003; 9:679–88. [PubMed: 13678446]
4. Silva GA, Czeisler C, Niece KL, Beniash E, Harrington DA, Kessler JA, et al. Selective differentiation of neural progenitor cells by high-epitope density nanofibers. Science. 2004; 303:1352–5. [PubMed: 14739465]
5. Engler AJ, Sen S, Sweeney HL, Discher DE. Matrix elasticity directs stem cell lineage specification. Cell. 2006; 126:677–89. [PubMed: 16923388]
6. Discher DE, Janmey P, Wang Y-l. Tissue cells feel and respond to the stiffness of their substrate. Science. 2005; 310:1139–43. [PubMed: 16293750]
7. Lutolf MP, Lauer-Fields JL, Schmoekel HG, Metters AT, Weber FE, Fields GB, et al. Synthetic matrix metalloproteinase-sensitive hydrogels for the conduction of tissue regeneration: Engineering cell-invasion characteristics. Proc Natl Acad Sci U S A. 2003; 100:5413–8. [PubMed: 12686696]
8. Dalsin JL, Hu BH, Lee BP, Messersmith PB. Mussel adhesive protein mimetic polymers for the preparation of nonfouling surfaces. J Am Chem Soc. 2003; 125:4253–8. [PubMed: 12670247]
9. Martino MM, Mochizuki M, Rothenfluh DA, Rempel SA, Hubbell JA, Barker TH. Controlling integrin specificity and stem cell differentiation in 2D and 3D environments through regulation of fibronectin domain stability. Biomaterials. 2009; 30:1089–97. [PubMed: 19027948]
10. Yang F, Murugan R, Wang S, Ramakrishna S. Electrospinning of nano/micro scale poly(L-lactic acid) aligned fibers and their potential in neural tissue engineering. Biomaterials. 2005; 26:2603–10. [PubMed: 15585263]
11. Bettinger CJ, Langer R, Borenstein JT. Engineering substrate topography at the micro- and nanoscale to control cell function. Angew Chem Int Ed. 2009; 48:5406–15.
12. Chew SY, Mi R, Hoke A, Leong KW. The effect of the alignment of electrospun fibrous scaffolds on Schwann cell maturation. Biomaterials. 2008; 29:653–61. [PubMed: 17983651]
13. Aubin H, Nichol JW, Hutson CB, Bae H, Sieminski AL, Cropek DM, et al. Directed 3D cell alignment and elongation in microengineered hydrogels. Biomaterials. 2010; 31:6941–51. [PubMed: 20638973]
14. Lim SH, Mao HQ. Electrospun scaffolds for stem cell engineering. Adv Drug Deliv Rev. 2009; 61:1084–96. [PubMed: 19647024]
15. Ji Y, Ghosh K, Shu XZ, Li B, Sokolov JC, Prestwich GD, et al. Electrospun three-dimensional hyaluronic acid nanofibrous scaffolds. Biomaterials. 2006; 27:3782–92. [PubMed: 16556462]
16. Coburn J, Gibson M, Bandalini PA, Laird C, Mao HQ, Moroni L, et al. Biomimetics of the extracellular matrix: An integrated three-dimensional fiber-hydrogel composite for cartilage tissue engineering. Smart Struct Syst. 2011; 7:213–22. [PubMed: 22287978]
17. Kang E, Choi YY, Chae SK, Moon JH, Chang JY, Lee SH. Microfluidic spinning of flat alginate fibers with grooves for cell-aligning scaffolds. Adv Mater. 2012; 24:4271–7. [PubMed: 22740066]
18. Kang E, Jeong GS, Choi YY, Lee KH, Khademhosseini A, Lee SH. Digitally tunable physicochemical coding of material composition and topography in continuous microfibres. Nat Mater. 2011; 10:877–83. [PubMed: 21892177]
19. Zhang S, Greenfield MA, Mata A, Palmer LC, Bitton R, Mantei JR, et al. A self-assembly pathway to aligned monodomain gels. Nat Mater. 2010; 9:594–601. [PubMed: 20543836]
20. Ji Y, Ghosh K, Li B, Sokolov JC, Clark RA, Rafailovich MH. Dual-syringe reactive electrospinning of cross-linked hyaluronic acid hydrogel nanofibers for tissue engineering applications. Macromol Biosci. 2006; 6:811–7. [PubMed: 17022092]
21. Nichol JW, Koshy ST, Bae H, Hwang CM, Yamanlar S, Khademhosseini A. Cell-laden microengineered gelatin methacrylate hydrogels. Biomaterials. 2010; 31:5536–44. [PubMed: 20417964]
22. Shu XZ, Liu Y, Palumbo FS, Luo Y, Prestwich GD. In situ crosslinkable hyaluronan hydrogels for tissue engineering. Biomaterials. 2004; 25:1339–48. [PubMed: 14643608]
23. Potter K, Balcom BJ, Carpenter TA, Hall LD. The gelation of sodium alginate with calcium ions studied by magnetic resonance imaging (MRI). Carbohyd Res. 1994; 257:117–26.

24. Cornwell KG, Pins GD. Enhanced proliferation and migration of fibroblasts on the surface of fibroblast growth factor-2-loaded fibrin microthreads. Tissue Eng Part A. 2010; 16:3669–77. [PubMed: 20673132]
25. Cornwell KG, Pins GD. Discrete crosslinked fibrin microthread scaffolds for tissue regeneration. J Biomed Mater Res A. 2007; 82:104–12. [PubMed: 17269139]
26. Sun JY, Zhao X, Illeperuma WR, Chaudhuri O, Oh KH, Mooney DJ, et al. Highly stretchable and tough hydrogels. Nature. 2012; 489:133–6. [PubMed: 22955625]
27. Onoe H, Okitsu T, Itou A, Kato-Negishi M, Gojo R, Kiriya D, et al. Metre-long cell-laden microfibres exhibit tissue morphologies and functions. Nat Mater. 2013; 12:584–90. [PubMed: 23542870]
28. Ingram DA, Mead LE, Tanaka H, Meade V, Fenoglio A, Mortell K, et al. Identification of a novel hierarchy of endothelial progenitor cells using human peripheral and umbilical cord blood. Blood. 2004; 104:2752–60. [PubMed: 15226175]
29. Bellan LM, Craighead HG. Molecular orientation in individual electrospun nanofibers measured via polarized Raman spectroscopy. Polymer. 2008; 49:3125–9.
30. Fennessey SF, Farris RJ. Fabrication of aligned and molecularly oriented electrospun polyacrylonitrile nanofibers and the mechanical behavior of their twisted yarns. Polymer. 2004; 45:4217–25.
31. Kongkhlang T, Tashiro K, Kotaki M, Chirachanchai S. Electrospinning as a new technique to control the crystal morphology and molecular orientation of polyoxymethylene nanofibers. J Am Chem Soc. 2008; 130:15460–6. [PubMed: 18950171]
32. Larson R, Mead D. The Ericksen number and Deborah number cascades in sheared polymeric nematics. Liq Cryst. 1993; 15:151–69.
33. Inai R, Kotaki M, Ramakrishna S. Structure and properties of electrospun PLLA single nanofibres. Nanotechnology. 2005; 16:208–13. [PubMed: 21727424]
34. Zong X, Kim K, Fang D, Ran S, Hsiao BS, Chu B. Structure and process relationship of electrospun bioabsorbable nanofiber membranes. Polymer. 2002; 43:4403–12.
35. Moon S, Ryu BY, Choi J, Jo B, Farris RJ. The morphology and mechanical properties of sodium alginate based electrospun poly(ethylene oxide) nanofibers. Polym Eng Sci. 2009; 49:52–9.
36. Angammana CJ, Jayaram SH. Analysis of the effects of solution conductivity on electrospinning process and fiber morphology. IEEE Trans Ind Appl. 2011; 47:1109–17.
37. Wagner C, Amarouchene Y, Bonn D, Eggers J. Droplet detachment and satellite bead formation in viscoelastic fluids. Phys Rev Lett. 2005; 95:164504. [PubMed: 16241806]
38. Tirtaatmadja V, McKinley GH, Cooper-White JJ. Drop formation and breakup of low viscosity elastic fluids: Effects of molecular weight and concentration. Phys Fluids. 2006; 18:043101.
39. Reneker DH, Yarin AL, Fong H, Koombhongse S. Bending instability of electrically charged liquid jets of polymer solutions in electrospinning. J Appl Phys. 2000; 87:4531.
40. Chae SK, Kang E, Khademhosseini A, Lee SH. Micro/nanometer-scale fiber with highly ordered structures by mimicking the spinning process of silkworm. Adv Mater. 2013; 25:3071–8. [PubMed: 23616339]

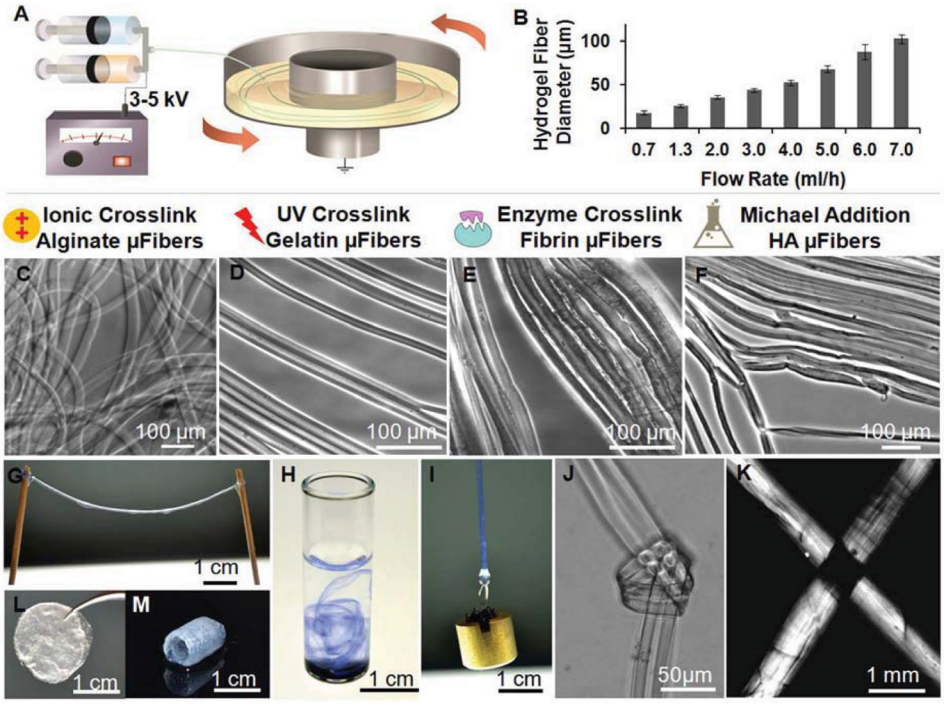

Fig. 1.

Electrostretching setup and features of hydrogel microfibres. (A) Illustration of the electrostretching setup. To prepare a dual component microfibres, two syringes (A & B) are used (e.g. sodium alginate solution in syringe A and fibrinogen solution in B) to mix the solutions prior to extrusion; a voltage of 3–5 kV was charged between the spinning solution and the collection bath. Typically only one syringe is needed for single solution spinning. (B) Effect of alginate solution feeding rate on the diameter of hydrogel microfibres. Alginate hydrogel microfibres with an average of 17–116 μm were prepared with a solution containing 2% sodium alginate and 0.2% PEO fed at a flow rate ranging from 0.7 to 7.0 ml/h. (C–F) Various crosslinking mechanisms have been employed to crosslink alginate, gelatin, fibrin and hyaluronic acid hydrogel microfibres. The crosslinking of the fibres was initiated with a fast calcium gelation of alginate, followed by additional crosslinking of the second component polymer with UV-initiated, enzymatic, or the Michael addition reaction for methylated gelatin, fibrin and hyaluronic acid, respectively. (G) Using this method, hydrogel microfibres of any desired length can be prepared. (H) When dispersed in water, alginate hydrogel fibres formed a loose network of hydrogel fibres. Trypan blue was used to stain the fibres and enhance observation. (I) A 10-g metal pillar was lifted with an alginate hydrogel microfibre bundle. (J) A micro-knot was made with two alginate hydrogel microfibres. (F) Under a cross polarized light microscope, light extinction was observed at the crossover point of two hydrogel microfibre bundles, indicating uniform alignment in both fibres. (L–M) Beyond microfibre bundles, these hydrogel microfibres can also be fabricated into other forms like fibrous films (L) and self-supporting hydrogel tubes (M).

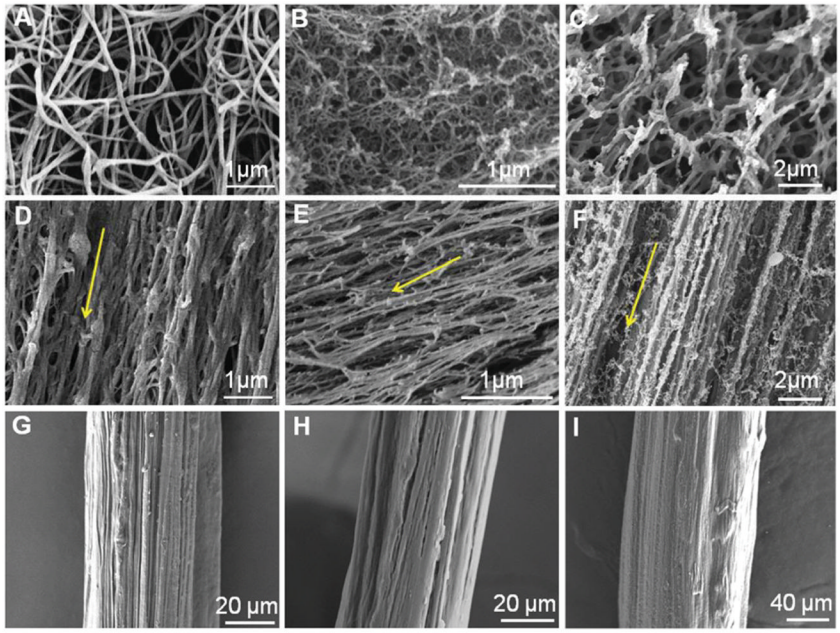

Fig. 2.

SEM micrographs of hydrogel fibres prepared with simple extrusion and electrostretching. (A–C) Fibrin (A), gelatin (B) and HA (C) hydrogels prepared by simple extrusion or mixing consist of randomly oriented nanofibre network. (D–F) Electrostretched fibrin (D), gelatin (E) and HA (F) hydrogel fibres showing preferential alignment. Arrows indicate the orientation of the microfibre longitudinal axis. (G–I) Fibrin (G), gelatin (H) and HA (I) hydrogel fibres following stretching and dehydration in air forming fibre bundles. Both fibrin and gelatin fibres preserved surface texture and grooves. Samples in (A–F) were prepared by the critical point drying technique; and samples in (G–I) were stretched and dried in air.

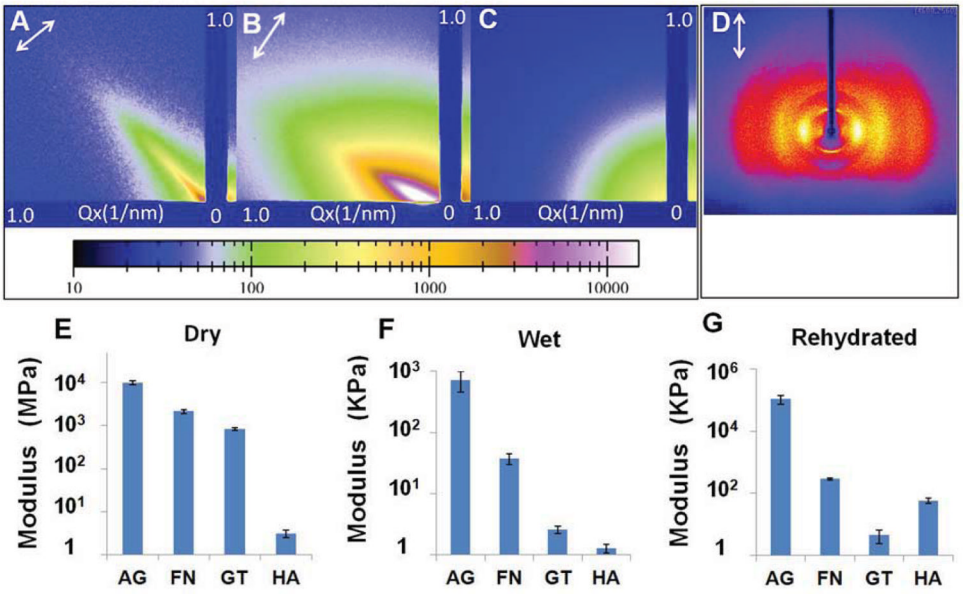

Fig. 3.

X-ray scattering diffraction patterns and tensile moduli of hydrogel fibres in dry and wet states. (A–B) Small angle X-ray scattering (SAXS) patterns of the dry (A) and wet (B) calcium alginate hydrogel fibres confirming an alignment axis along the microfibre orientation indicated by the arrows. (C) SAXS pattern of alginate hydrogel prepared by hand extrusion suggesting an isotropic structure. (D) Wide angle x-ray scattering pattern of the dry alginate microfibres confirming the polymer chain alignment along the fibre axis as indicated by the arrow. (E–G) Tensile moduli of alginate (AG), fibrin (FN), gelatin (GT) and hyaluronic acid (HA) hydrogel fibres in dry (E), wet (F) and rehydrated form (G).

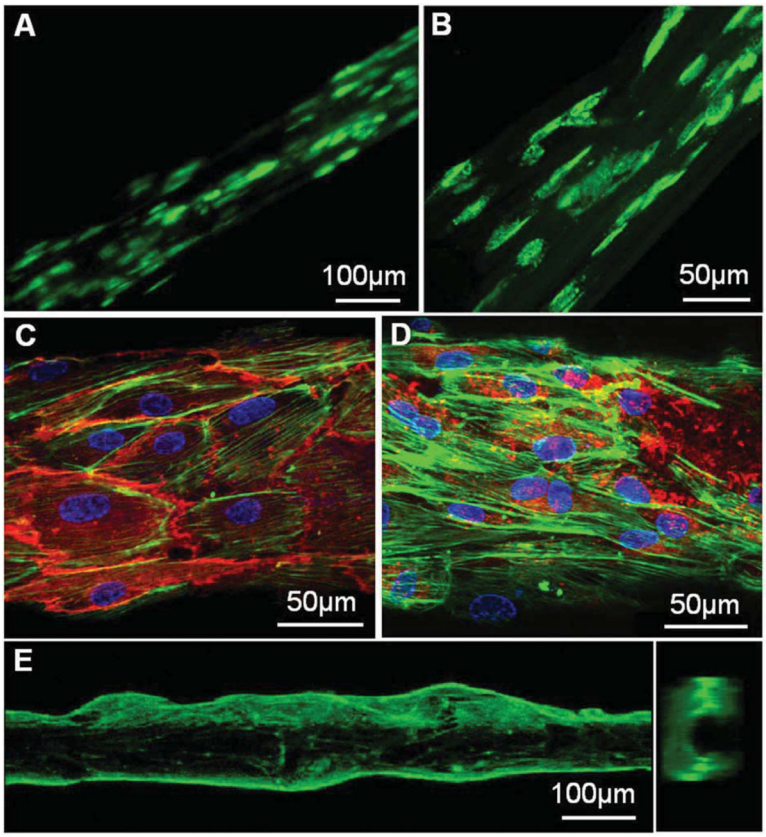

Fig. 4.

Fluorescence micrographs of cells grown inside or outside fibrin hydrogel microfibres. (A–B) ASCs with CellTracker™ green CMFDA dye were encapsulated in 0.75 wt% fibrin hydrogel fibres. After 2 days (a) and 5 days (b) of culture, cells spread out showing alignment along the fibre axis. (C–D) F-actin filament (green) staining of human ECFCs cultured on the surface of a rehydrated fibrin microfibre, overlapped with immunofluorescence staining for CD31 (red) (C) or vWF (red) (D) and DAPI (blue) staining for cell nuclei. (E) A side view and a cross-section view of the sample shown in (C–D), indicating that the differentiated ECFCs grew into a confluent tubular structure.

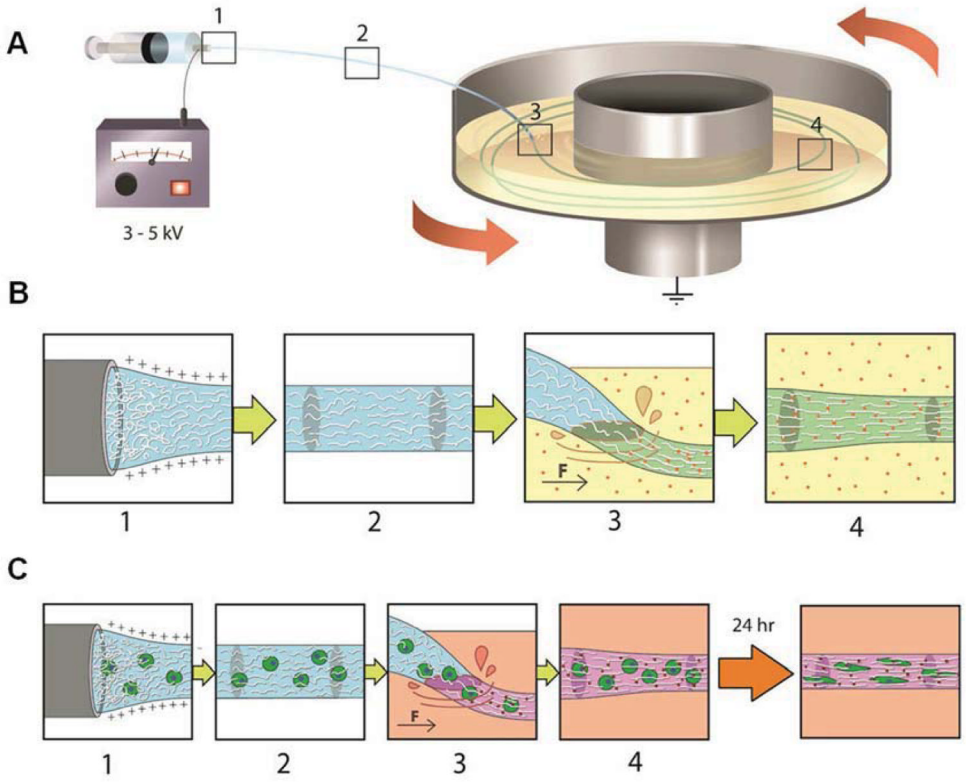

Fig. 5.

Illustration of polymer alignment as a result of electrical and mechanical stretching. (A–B) Spinning of alginate hydrogel fibres is illustrated here as an example. Sodium alginate polymer chains in the aqueous solution are increasingly aligned as the solution jet is extruded from the needle tip (Box 1) and stretched during traveling (Box 2) to the receiving bath. Under the effect of mechanical stretching as the alginate solution jet lands in the rotating bath (Box 3) containing calcium ions (red dots), alginate chains are further aligned and the crosslinked by calcium ions in the bath (Box 4), forming stable hydrogel microfibers. Other crosslinking methods (e.g. enzymatic, UV-initiated, or chemical reactions) can be used instead of, or in addition to, calcium-induced crosslinks (Boxes 3 and 4). (C) Cells can be incorporated in the spinning solution, and spun using the same method as shown in (B). The encapsulated cells sense and become elongated along the axial alignment direction, forming “cellular strings”.

Table 1

Spinning parameters for different hydrogel microfibers.

Hydrogel Composition	Spinning Solution Concentration (wt%)	Crosslinking Method	Crosslinking Condition
Alginate	0.75–3.0% Alginate 0.1–0.4% PEG	Ionic crosslinking	25–100 mM $CaCl_2$
Fibrin + Alginate	0.67–2.0% Fibrin 0.25–2.5% Alginate 0.1–0.2% PEG	Enzymatic & ionic crosslinking	5 U/ml thrombin 50 mM $CaCl_2$
Gelatin + Alginate	1.0–3.2% Gelatin 0.24–0.86% Alginate 0.40–1.0% Irgacure	Ionic & UV-crosslinking	50 mM $CaCl_2$ 0.50% Irgacure 10 min UV at 365 nm
Hyaluronic Acid + Alginate	1.0–2.0% HA 1.5% Alginate 0.1–0.4% PEG	Ionic & Michael-Addition crosslinking	1% PEGDA & 50 mM $CaCl_2$

All hydrogel microfibres were spun at 3–5 kV electrical potential and collected in a receiving bath spun at 25–80 rpm.